OXFORD

ORIGINAL ARTICLE

Interactome analysis reveals that FAM161A, deficient in recessive retinitis pigmentosa, is a component of the Golgi-centrosomal network

Silvio Alessandro Di Gioia[1,†], Pietro Farinelli[1,†], Stef J.F. Letteboer[3], Yvan Arsenijevic[2], Dror Sharon[4], Ronald Roepman[3] and Carlo Rivolta[1,*]

[1]Department of Medical Genetics, University of Lausanne, Lausanne, Switzerland [2]Unit of Gene Therapy and Stem Cell Biology, Jules-Gonin Eye Hospital, University of Lausanne, Lausanne, Switzerland, [3]Department of Human Genetics and Nijmegen Centre for Molecular Life Sciences, Radboud University Nijmegen Medical Centre, Nijmegen, The Netherlands and [4]Department of Ophthalmology, Hadassah-Hebrew University Medical Center, Jerusalem, Israel

*To whom correspondence should be addressed at: Department of Medical Genetics, University of Lausanne, Rue du Bugnon 27, 1005 Lausanne, Switzerland. Tel: +41 216925451; Fax: +41 216925455; Email: carlo.rivolta@unil.ch

Abstract

Defects in FAM161A, a protein of unknown function localized at the cilium of retinal photoreceptor cells, cause retinitis pigmentosa, a form of hereditary blindness. By using different fragments of this protein as baits to screen cDNA libraries of human and bovine retinas, we defined a yeast two-hybrid-based FAM161A interactome, identifying 53 *bona fide* partners. In addition to statistically significant enrichment in ciliary proteins, as expected, this interactome revealed a substantial bias towards proteins from the Golgi apparatus, the centrosome and the microtubule network. Validation of interaction with key partners by co-immunoprecipitation and proximity ligation assay confirmed that FAM161A is a member of the recently recognized Golgi-centrosomal interactome, a network of proteins interconnecting Golgi maintenance, intracellular transport and centrosome organization. Notable FAM161A interactors included AKAP9, FIP3, GOLGA3, KIFC3, KLC2, PDE4DIP, NIN and TRIP11. Furthermore, analysis of FAM161A localization during the cell cycle revealed that this protein followed the centrosome during all stages of mitosis, likely reflecting a specific compartmentalization related to its role at the ciliary basal body during the G_0 phase. Altogether, these findings suggest that FAM161A's activities are probably not limited to ciliary tasks but also extend to more general cellular functions, highlighting possible novel mechanisms for the molecular pathology of retinal disease.

Introduction

The Golgi apparatus (GA) is classically defined as a fundamental component of the cellular secretory pathway, where proteins synthesized in the endoplasmic reticulum are post-translationally modified prior to their export to the cell membrane or to lysosomes. Recent research has shown, however, that this organelle is also critical for correct microtubule (MT) organization and ciliogenesis, via mechanisms that are not yet fully understood (1). For instance, increasing evidences indicate that the GA can integrate the radial arrays of MTs originating from the centrosome (2) and may be itself a MT organizing center (MTOC) acting independently from the centrosome (3). A number of proteins involved in MT nucleation are also shared between the centrosome and this

organelle, suggesting the existence of common functions (1). Furthermore, it has been shown that preservation of GA ribbons is necessary for proper ciliogenesis, and that many ciliary components are indeed present in the GA (4).

The MT network is an array of tracks along which intracellular components are trafficked within the cell body. Additionally, the MT network establishes communications between different cellular compartments, including the GA and the centrosome (5). In cells of higher eukaryotes, the GA is placed pericentrosomally. However, its localization within the cell is significantly altered during mitosis, when Golgi membranes are fragmented and dispersed throughout the cytoplasm to ensure equal redistribution to the daughter cells (6). At G_0, the centrosome migrates towards the cell surface and, after docking on the plasma membrane, the mother centriole of the centrosome is converted into a basal body from which the primary cilium originates (7).

The cilium is an almost ubiquitous, hair-like organelle involved in several functions, such as signaling (8), cell motility (9), environment and mechano-sensing (7,10) and embryonic development (11). These multifaceted functions render it one of the most intensively studied subcellular structures over the past few years (12).

Ciliopathies are an emerging class of diseases caused by mutations in genes that encode for proteins of the cilium. They include a broad spectrum of disorders affecting one or several tissues and organs, including kidney, skin, brain, bones and retina (13). Retinal degeneration is one of the major hallmarks of ciliopathies, and sometimes it is the sole phenotype (13–15). Among retinal ciliopathies, retinitis pigmentosa (RP) is the most prevalent condition (16). This disease is characterized in patients by the progressive degeneration of both rod and cone photoreceptors, the light-sensing cells of our eyes. Typically, patients gradually lose vision over many years, initially in the mid-periphery of their visual field, and subsequently in the periphery and the center, according to a rod–cone pattern of degeneration. As the condition progresses, only tiny islands of vision are left, and patients may eventually become legally or completely blind (17). RP is a Mendelian disease with a high genetic heterogeneity (18), caused by mutations in any of over 50 genes, many of which encode ciliary components. Examples of those genes include *RP1*, *C2orf71*, *RPGR*, *RPGRIP1*, *CEP290* and *KIZ*, all of which code for proteins involved in protein transport and maintenance of the photoreceptor's connecting cilium, axoneme and basal body (15,19–22).

FAM161A is a ciliary protein of unknown function, the loss of which causes recessive RP (23,24). It contains three coiled-coil regions, two of which are part of the UPF0564 domain, a well-conserved structure that has been defined by *in silico* analyses but that still lacks a precise functional characterization. The *FAM161A* gene is frequently mutated in patients from Israel (24), although it can be associated with the disease in other regions of the world as well (23,25,26). All mutations in *FAM161A* identified so far lead to premature stop codons that seem to trigger nonsense mediated decay of mutant mRNA and thus result in the absence of FAM161A in affected patients (25). We and others have shown that FAM161A localizes at the connecting cilium and ciliary basal body of rodent and human photoreceptors (27,28), and binds to and possibly stabilizes MTs (28). In addition, FAM161A interacts with other proteins involved in retinal ciliopathies and localizes at the basal body in ciliated cell lines (27); recently, mutations in the basal body protein POC1B were found to disrupt its interaction with FAM161A (29). Also, the inhibition of *FAM161A* expression via siRNA partly impairs formation of the cilium (27). Furthermore, in *Fam161a*[GT/GT] mice photoreceptors showed shortened connecting cilia, and spread ciliary MT doublets (30). However, the inclusion and precise positioning of FAM161A within the ciliary protein network (31), strongly suggested by its role in the etiology of retinal degeneration, has not yet been determined.

In this work, we unveil the binary interactome of FAM161A by GAL4-based yeast two-hybrid (Y2H) screening of bovine and human retinal cDNA libraries, and validate these findings by immunoprecipitation and proximity ligation assays. Specifically, we find that FAM161A directly interacts with several proteins from a GA-centrosome subcellular pathway, likely to be involved in the control of MT nucleation and in the transport of cellular components along the cytoskeleton, as well as in the regulation of ciliogenesis and maintenance of cell stability.

Results

Yeast two-hybrid screening assays reveal novel FAM161A interactors

Previous data have shown that FAM161A may interact with other proteins, preferentially via its C-terminal moiety containing the UPF0564 domain (27,28). However, it is not clear whether UPF0564 can exert its binding functions in an autonomous way with respect to the rest of the protein and whether other parts of FAM161A are involved in interaction processes independently from this domain. In our Y2H experiments, we therefore used three distinct FAM161A baits (FAM161A full length, FAM161A-N-term and FAM161A-C-term, containing the UPF0564 sequence, Supplementary Material, Fig. S1) (27) to initially screen an oligo dT-primed human retinal cDNA library.

After yeast transformation, we selected ∼500 positive clones, which were re-streaked on new plates containing selective medium. Of these, 297 passed the alpha- and/or beta-galactosidase colorimetric assays, including 247 colonies identified with the full-length bait, 37 with the C-term bait and 13 with the N-term bait (Supplementary Material, Table S1). Repeated colony PCRs on sequences from the prey plasmids yielded amplification products for more than half of them, giving a total of 162 sequenceable substrates. We revealed 101 (77%) true positives (prey-encoding sequence in-frame with the GAL4-AD) for the full-length bait, 18 (78%) for the C-term bait, yet surprisingly, none for the N-term bait. To enhance the resolution of the screening towards N-terminal domains that can be sterically hindered from detection in the oligo dT-primed library screen, we performed a second round of experiments with the full-length FAM161A and C-term encoding bait constructs, using a randomly primed prey cDNA library from bovine retina (Supplementary Material, Table S1).

Sanger sequencing of these colonies and validation of the reading frame of the detected preys allowed identifying 53 different putative interactors of FAM161A (Supplementary Material, Tables S2 and S3), including FAM161A itself and a number of proteins previously found to be associated with ciliopathies or interacting with ciliary proteins. Twenty-three out of these 53 hits (43%, Supplementary Material, Table S3) were entries in the ciliary proteome database (32). Within the set of FAM161A interactors discovered by Y2H, ciliary proteins showed indeed a highly statistically significant over-representation (hypergeometric P-value $= 3.6 \times 10^{-7}$, determined as: 23/53 versus 2726 entries in the ciliary database/18 523 entries in Swissprot; Fold enrichment $= 2.9$) (32,33). Network analysis of these interactors using GeneMANIA (34) showed a clear interconnection between many of the identified proteins, with just a few outliers (Fig. 1 and Supplementary Material S1).
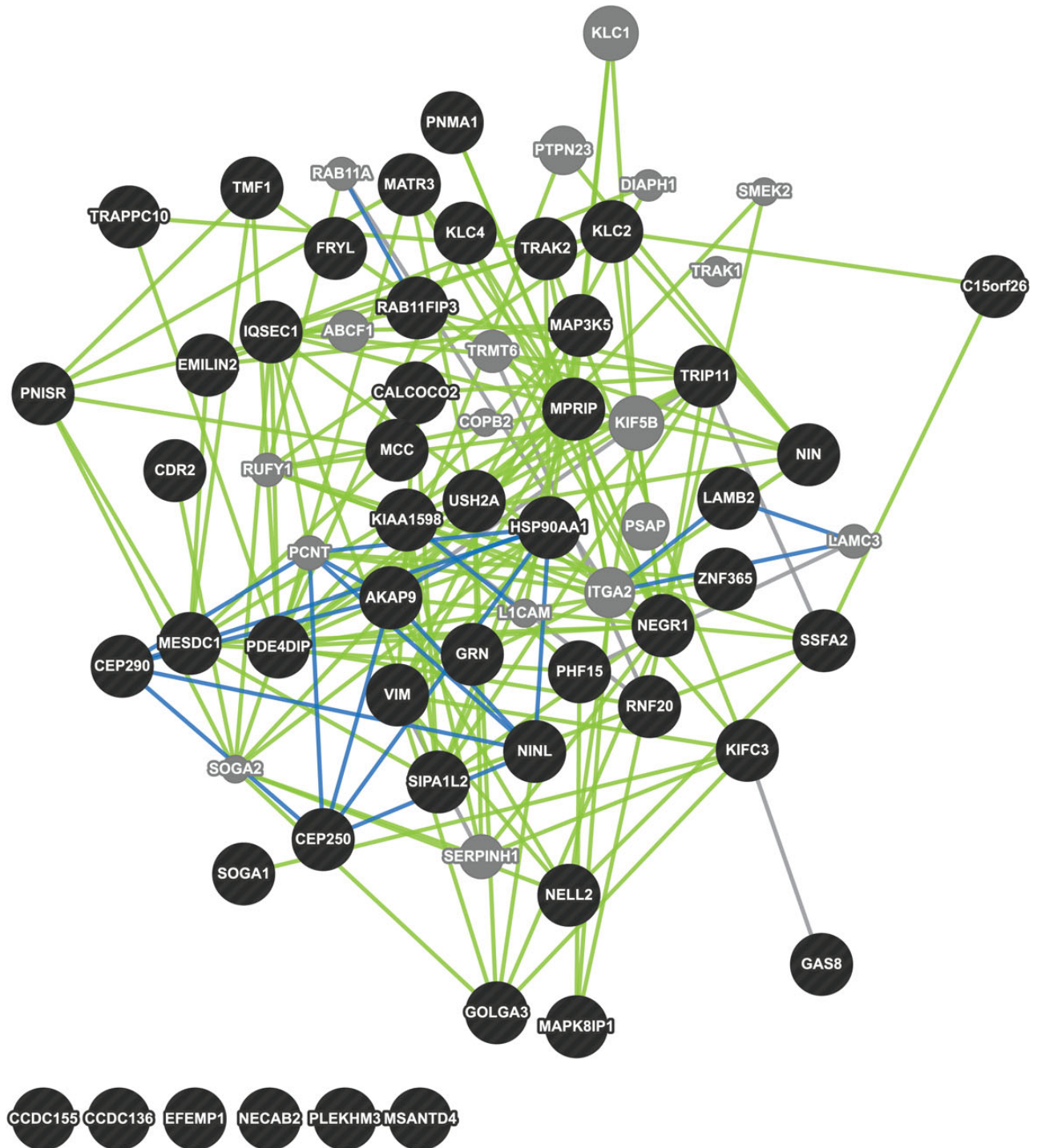
Figure 1. Network analysis of FAM161A interactors, following sequencing of positive Y2H clones and the use of the GeneMANIA algorithm. The results obtained show a dense pattern of relationships. Each circle indicates a gene/protein. Black circles indicate elements identified by the Y2H assay, whereas grey circles indicate interactors that were not identified by this screening but could link two experimentally determined interactors. Blue lines connect proteins belonging to the same pathway, green lines show genetic interaction, while grey lines highlight proteins with shared domains. Genes/proteins that could not be integrated in this network are aligned at the bottom.

Interactors belong to three distinct but interconnected subcellular components

Gene ontology (GO) analysis (35,36) of the 53 FAM161A interactors showed an enrichment of proteins that are present within the MT cytoskeleton, centrosome and cilium, as well as the GA, with

significant P-values. Additionally, GO classification according to molecular function indicated a clear bias towards MTs, cytoskeleton, centrosome and MTOCs (Supplementary Material, Table S4). A more detailed analysis of the literature revealed that many of these interactors could be separated in three
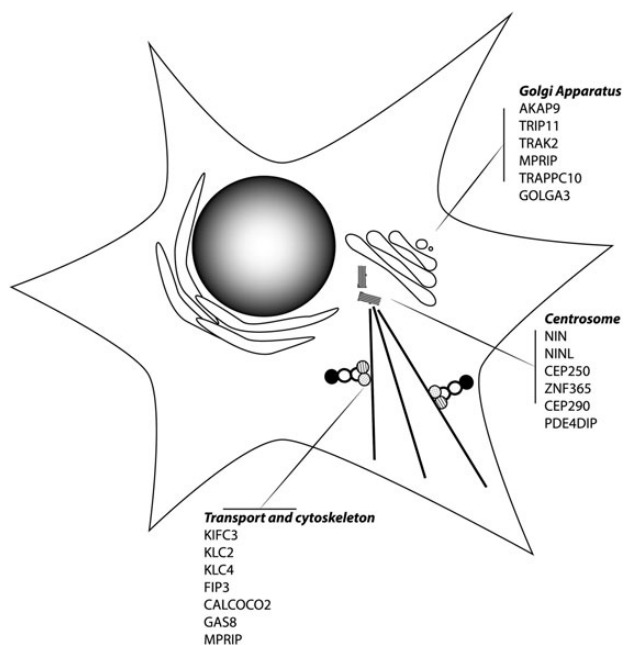
Figure 2. Schematic representation of a cell and localization of FAM161A's interactors, as reported in the literature. Separation of interacting proteins within the Golgi, the centrosomal and the cytoskeletal networks is highlighted. The thick black straight lines indicate the microtubule network and the cartoons lying on them schematize microtubule motor proteins.

different subgroups: (i) proteins that localize at the GA and are in strict contact with the MT network, (ii) centrosomal proteins and (iii) proteins belonging to the cytoskeletal transport network (Fig. 2). Taken together, these results suggested that FAM161A is part of the Golgi-centrosomal network.

Based on these data and on previous findings showing that FAM161A natively co-localizes with the centrosome/basal body in G_0 photoreceptors and in ciliated cells (27), we wanted to observe the behavior of FAM161A during the cell cycle. Co-staining of FAM161A and glutamylated tubulin showed that indeed FAM161A followed the centrosome throughout all phases of mitosis in hTERT-RPE1 cells (Fig. 3).

Co-immunoprecipitation confirms interaction of FAM161A with components of the Golgi apparatus, cytoskeletal and centrosomal networks

To validate the interactions observed with the Y2H assay, we performed IP experiments using antibodies that could bind newly discovered FAM161A partners. We selected proteins for each of the three different categories of interactors described above, depending on the commercial availability of antibodies and whether they were suitable for IP (based on the information available in the literature or in products' data sheets). For these experiments, we used plasmids expressing the same FAM161A portions as for the Y2H experiments, fused to a Flag tag at their N-terminal parts (27). As a negative control, we used a plasmid expressing a flagged non-functional form of the nuclear protein SOX4. All constructs yielded significant protein production upon transfection into HEK293T and HeLa cells.

For each protein of interest, we performed reciprocal co-immunoprecipitations (Co-IP), using either an antibody directed against the FAM161A interactor, or against the Flag epitope of the recombinant protein (Fig. 4). Concerning the first group of interactors, i.e.

GA proteins, we efficiently immunoprecipitated GOLGA3 and revealed the presence of FAM161A full length. The reciprocal experiments confirmed these findings, highlighting interaction with the same construct and with FAM161A-C-term (Fig. 4A).

Representing the centrosomal proteins (second group), we could reciprocally confirm interaction with ninein (NIN). Signals originated only from experiments in which full-length FAM161A was tested, either as a protein to be revealed following IP of NIN or as a bait protein to be immunoprecipitated and reveal NIN (Fig. 4B).

Proteins from the third group of interactors (cytoskeletal transport), namely KIFC3 and KLC2, could both co-immunoprecipitate FAM161A full length and FAM161A-C-term, as revealed by anti-Flag reactivity on western blots (Fig. 4C). However, the reciprocal experiments showed absence of signals in all tests, probably reflecting a phenomenon of epitope masking by the anti-Flag antibody (not shown).

Finally, we tested interaction between FAM161A and AKAP9, a key protein that functionally links the GA with the centrosome (4), to further support the idea that FAM161A could indeed be part of the Golgi/centrosomal network. Despite AKAP9's high molecular weight, we could efficiently immunoprecipitate it and clear positive signals were detected in both direct and reciprocal experiments, when full-length FAM161A was used (Fig. 4D).

Proximity ligation assay

To circumvent limitations of these IP experiments, due to both availability of efficient immunoprecipitating antibodies and their potential stereochemical encumbrance preventing detection of prey proteins, we adopted an alternative approach to verify binding between FAM161A and other proteins of the Golgi-centrosomal network. Specifically, we used the proximity ligation assay (PLA), a relatively recent technique that enables the *in situ* identification of protein–protein interaction by detecting physical proximity of antibodies targeting two protein partners.

Using this technology, we found statistically significant DNA amplification and fluorescence for all eight FAM161A interactors that were tested, namely AKAP9, FIP3, GOLGA3, KIFC3, KLC2, PDE4DIP (Myomegalin), NIN and TRIP11 (GMAP210) (Fig. 5, Table 1 and Supplementary Material, Fig. S2), compared with specific controls (highest $P = 4 \times 10^{-3}$; lowest $P < 1 \times 10^{-4}$; highest $n = 258$; lowest $n = 126$ measured cells per assay per condition).

Discussion

We and others have recently demonstrated that FAM161A is a new ciliary protein (27,28) interacting with a number of other proteins associated with human ciliopathies (27). In this work, we used Y2H screening as a high-throughput technique to identify additional FAM161A molecular partners in the mammalian retina. This approach allowed the identification of as many as 53 distinct possible interactors and revealed that FAM161A belongs to three functional compartments, i.e. the Golgi/MT, the cytoskeletal/transport and centrosomal networks.

In our approach, we used three distinct FAM161A sequences to screen for molecular partners expressed in human or bovine retinas. Interestingly, we obtained reliable data only when the full length or the C-terminal portion of FAM161A was used, with a clear bias for the former construct over the latter one in terms of the number of positive clones/colonies (132 versus 23 and 94 versus 33 for human and bovine libraries, respectively). These data suggest that the UPF0564 domain, contained in the C-term moiety of the FAM161A, is necessary to establish protein–protein interactions. However, these results also imply
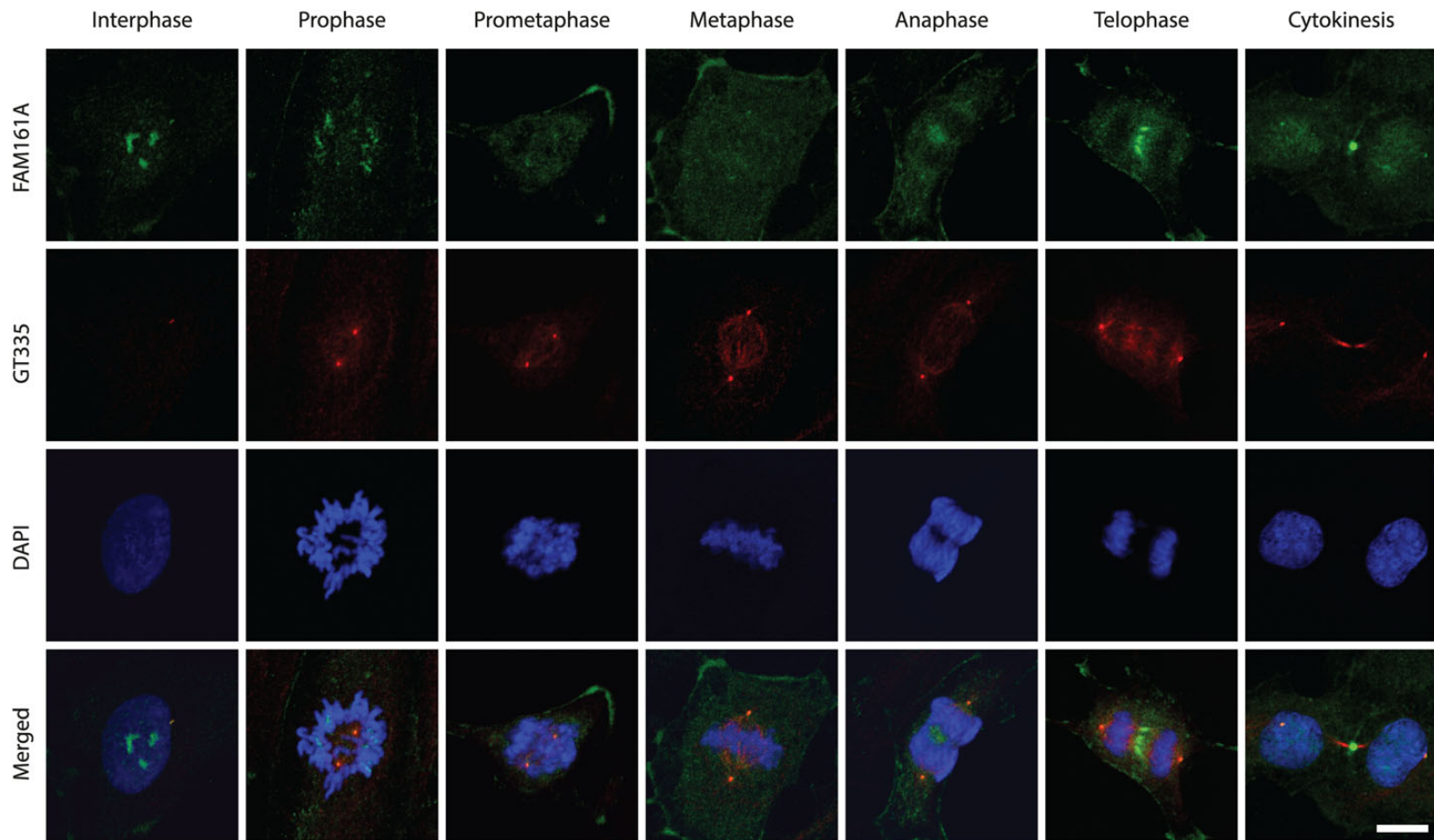
Figure 3. FAM161A localization during mitosis, in hTERT-RPE1 cells. Native FAM161A localization within the cell is indicated by green fluorescence, while GT335 (red) stains the centrosome and mitotic spindle microtubules. DAPI blue fluorescence reveals the presence of cell nuclei. Merged channels are shown in the bottom panels. Scale bar: 10 μm.
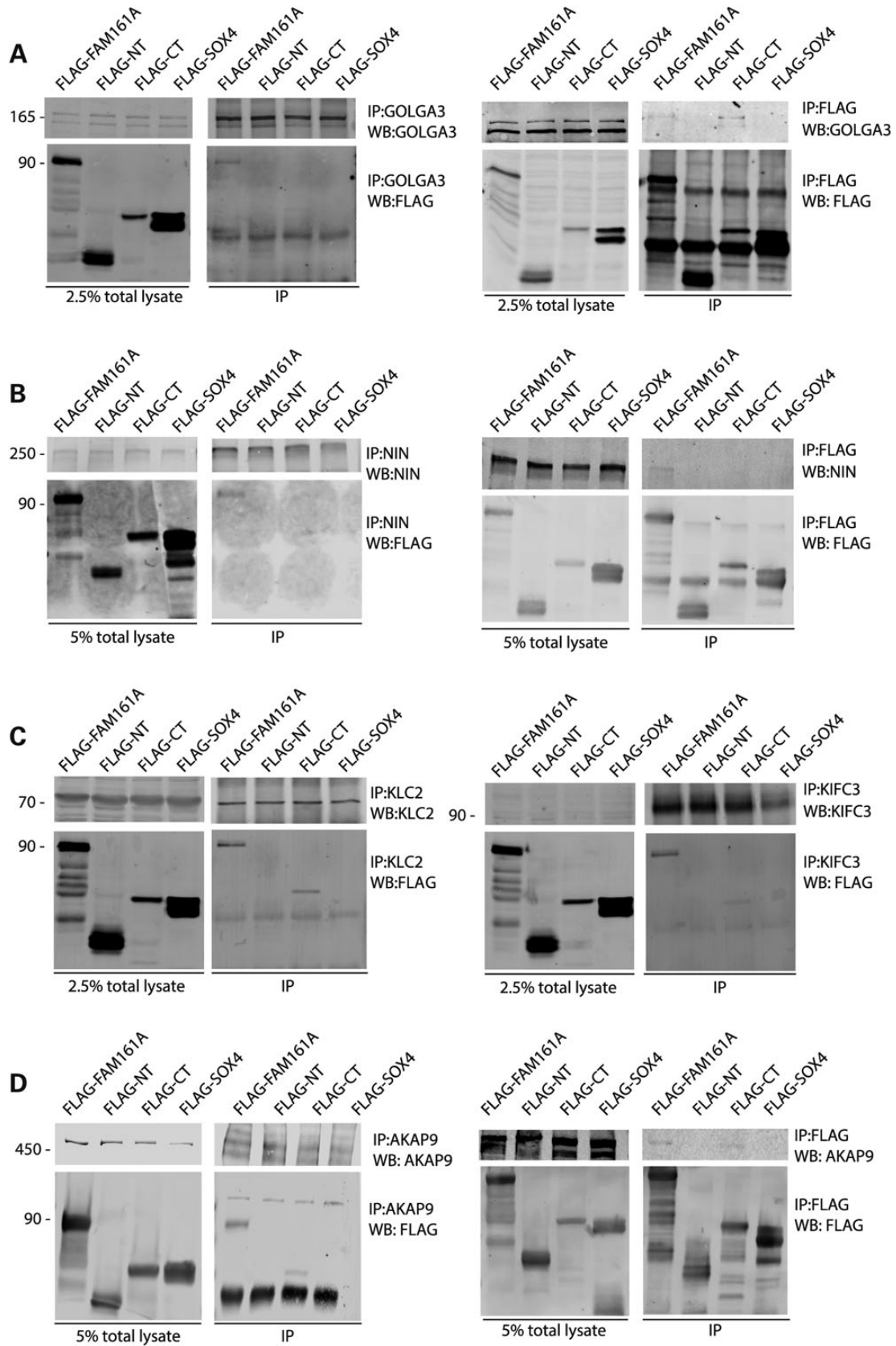
Figure 4. Co-immunoprecipitation of portions of FAM161A and endogenous interactors. Every panel shows the expression of the native protein (top left) and of different FAM161A Flag-tagged constructs (bottom left) in HEK293T cells, as well as the presence of the same proteins in immunoprecipitated samples (right panels). IP:x, protein or peptide targeted by the antibody used in immunoprecipitation; WB:x, protein or peptide targeted by the antibody used in western blots, NT, N-terminal portion of FAM161A; CT, C-terminal portion of FAM161A; SOX4, negative control for immunoprecipitation. Numbers on the left of panels indicate molecular weight (in kDa).
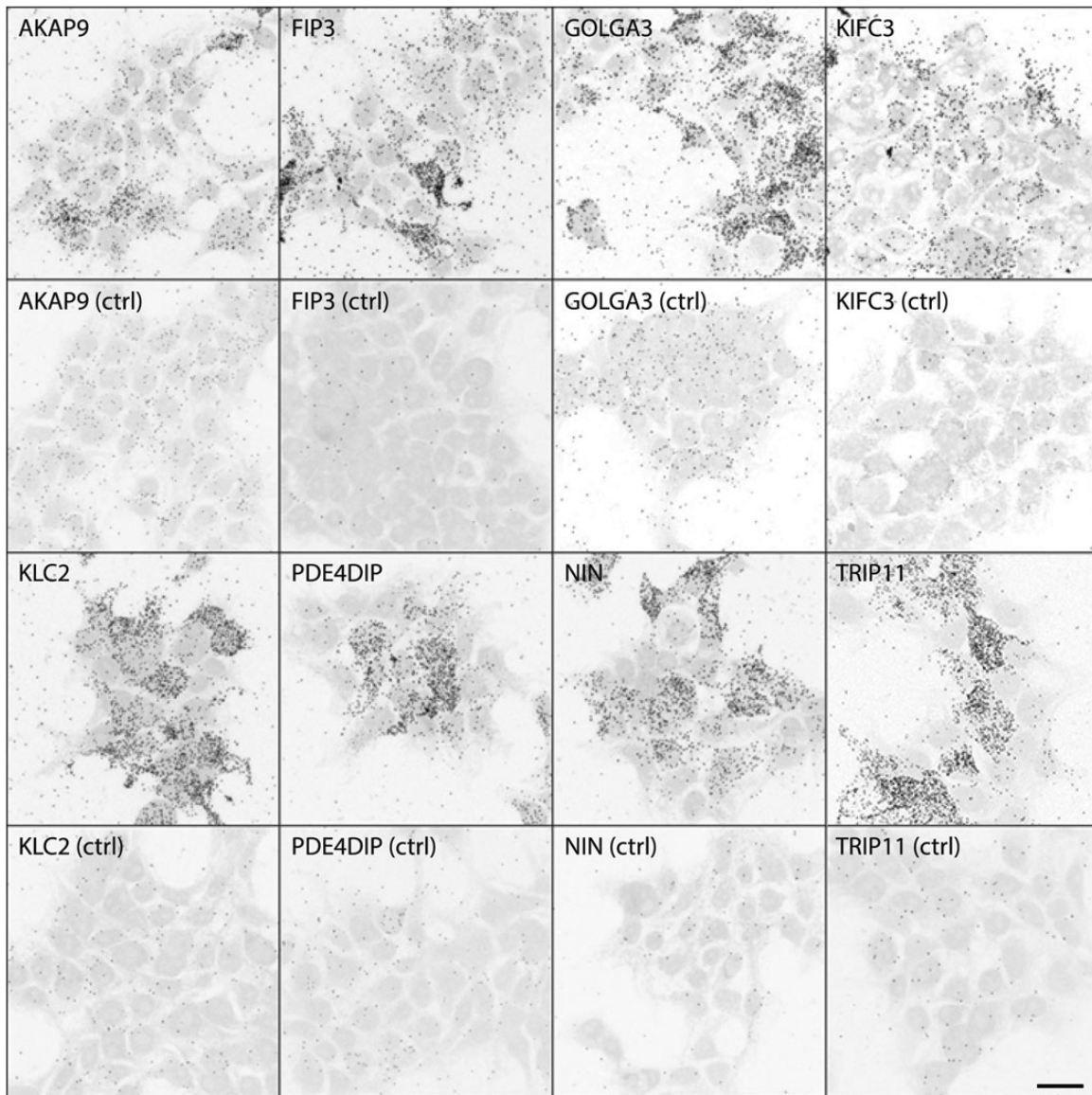
Figure 5. Representative images of proximity ligation assays assessing interaction between Flag-FAM161A and endogenous proteins in HEK293T cells. Black dots indicate *in situ* proximity/interaction. The protein assessed for interaction with FAM161A and its respective negative control (ctrl) is reported in each panel. Cells' nuclei appear in grey. Scale bar: 20 μm.

that the presence of the N-terminal portion of FAM161A containing the first coiled-coil domain may be required for strengthening or perhaps even determining the specificity of UPF0564-mediated interactions. Indeed, most, but not all the preys captured by the full-length FAM161A bait were captured by the C-term construct.

The relatively large number of identified interactors suggests that FAM161A can act as a scaffold, probably exerting its function(s) in multiple protein complexes. In addition, functional classification assigns these molecular partners a role in cytoskeletal and microtubular activities, in agreement with previous findings (27,28,30).

Interestingly, the three major classes of proteins to which FAM161A interactors belong are themselves interconnected. It has been clearly shown, for example, how Golgi ribbons are physically located in proximity of centrosomes in interphase eukaryotic cells (37). This localization is mediated by several proteins, such as golgins and GRASPs (38). In agreement with these data, we found GOLGA3, a protein belonging to the golgin family, as a new FAM161A interactor. GOLGA3 is thought to accomplish a number of tasks, including the recruitment of dynein motor proteins to the GA (39), suggesting that FAM161A may be involved in intracellular transport.

Furthermore, the formation of the primary cilium requires the interaction between the GA and the centrosome. In eukaryotes, during ciliogenesis centrosomes migrate from the Golgi area to the proximity of the apical plasma membrane, where they undergo a transition into a basal body and participate in the genesis of primary cilium (40). A critical component of ciliogenesis, IFT20, localizes at the Golgi and interacts with the Golgi protein GMAP210 (41) (whose gene is called *TRIP11*), which we identified as a FAM161A interactor in our study. Moreover, cilium formation

Table 1. Quantitative results of PLA experiments

Interactor	Experiment[a]	Control[a]	P-value
AKAP9	48.98 ± 5.76; 174	15.41 ± 0.67; 159	0.0002
FIP3	98.26 ± 18.15; 175	1.26 ± 0.21; 258	0.0007
GOLGA3	93.71 ± 12.00; 154	19.26 ± 2.37; 239	0.0003
KIFC3	23.57 ± 5.25; 194	2.64 ± 0.19; 171	0.004
KLC2	70.74 ± 13.91; 147	6.73 ± 1.15; 151	0.0018
PDE4DIP	72.17 ± 4.30; 168	7.77 ± 0.83; 209	<0.0001
NIN	45.87 ± 4.38; 126	3.04 ± 0.83; 163	<0.0001
TRIP11	42.50 ± 8.41; 150	2.16 ± 0.31; 205	0.0014

[a]Measured events × cell (average ± standard error of the mean); number of cells measured.

requires proteins that are produced in the Golgi, and Golgi ribbons specifically localize in proximity of the centrosome. Destruction of Golgi ribbons, which are localized in proximity of the centrosome, impairs ciliogenesis and cell migration (4). One of the key components for the maintenance of the Golgi ribbon structure in relationship with the centrosome is AKAP9 (4). We observed a direct interaction of FAM161A and AKAP9 and confirmed this interaction by immunoprecipitation and PLA. It has recently been observed that AKAP9 is also able to bind to γ-tubulin and participates in the nucleation and elongation of MTs from the centrosome and that its depletion also impairs ciliogenesis (42). In addition, AKAP9 can recruit PDE4DIP, another FAM161A interactor that we revealed in this study, at the centrosome (43). Finally, the GMAP210 protein, mentioned above, acts as a homodimeric protein able to bind the minus-end of MTs and γ-tubulin, which is indispensable for the Golgi architecture (44). Therefore, the correct localization of AKAP9, GOLGA3 and GMAP210 at the Golgi and/or centrosome is necessary for the cell to accomplish the basic functional tasks required during differentiation and cellular polarization.

The second class of FAM161A's interactors identified in this screening are *bona fide* centrosomal proteins and many of these are involved in mitosis. Among centrosomal FAM161A interactors, two of the main players are NIN and AKAP9, which are also expressed at the Golgi (45). In association with CEP110 and CEP250, NIN is also fundamental for the formation of the MTOCs at the centrosome and for centrosome maturation (46). NIN anchors the minus-end of the MT at the subdistal appendage of the mother centriole of the centrosome and directly interacts with γ-tubulin at the same position (47). Moreover, NIN is capable of anchoring minus-end MTs at non-centrosomal sites, acting itself as a MTOC (48). NIN also participates in mitosis by directly interacting with Astrin and the reduction of NIN levels leads to the formation of an aberrant mitotic spindle (49). Although we observe the constant co-localization of FAM161A and the centriole during the cell cycle and mitosis, it is unlikely that FAM161A has an essential role in this latter cellular process at a systemic level, since the complete absence of this protein in human individuals is non-fatal (23,24). Therefore, this specific localization may not indicate *per se* a real function during cell division, but simply reflect specific compartmentalization, also observed for other ciliary proteins without any clear role in mitosis (50,51). Alternatively, specific FAM161A's function at mitosis may exist, but could be redundant with respect to that of other proteins, notably of its paralogue and UPF0564-containing FAM161B (28).

It has also been shown previously that NIN is crucial for ciliogenesis (52), and that in cells where cilium formation was prevented NIN did not localize at the basal body (53). Furthermore, NIN co-localizes with the centrosomal protein CEP250 (46),

another putative interactor of FAM161A, as ascertained in our Y2H assay. It is interesting to observe that the knockdown of either CEP250 or NIN reduce primary cilium formation (54), similar to that observed with FAM161A depletion (27), and that a nonsense mutation in CEP250 was identified in patients with Usher syndrome (55). In addition to AKAP9 and PDE4DIP, three additional proteins involved with MT anchoring at the centrosome (CDK5RAP2, CAP350 and pericentrin) are associated with the GA (56–58). It would not be surprising if these proteins, that were not present in our Y2H screening, would later be revealed as FAM161A interactors.

Intracellular transport of macromolecules is a fundamental cellular function and generally relies on motor proteins. Kinesins are MT-associated motor proteins involved in the anterograde transport (from the minus-end to the plus-end) of intracellular components (59). In our Y2H study, we were able to identify interactions between FAM161A and different kinesins, including KLC2, which is a component of the light chain subunit of the heterotetrameric Kinesin-I subfamily (KIF5A, B and C). Kinesin-I motor proteins have been shown to participate in the intracellular transport of neurotrophins intraocularly injected into chicken eyes (60). KLC2 is expressed ubiquitously and has, *per se*, no motor activity but binds the SMAD2 cargo following its phosphorylation by GSK3β (61). Additionally, GSK3β-dependent phosphorylation of KLC2 plays an important role in the trafficking of AMPA receptors (62). GSK3β is also able to phosphorylate NIN promoting its oligomerization (63). Therefore, it seems conceivable that the functions of FAM161A are either directly or indirectly affected by GSK3β.

By showing that the C-terminal kinesin KIFC3 also interacts with FAM161A, we demonstrate here that binding of FAM161A to motor proteins is not limited to kinesin light chains. C-terminal kinesins are regarded as atypical, because, unlike the other members of the family, they are MT minus-end-directed motors (64). KIFC3 is ubiquitously present throughout the human body (65) and is abundantly expressed in the human retinal pigment epithelium and in the outer plexiform layer of the retina (66). KIFC3 is also important for GA positioning and structure maintenance (67) and recent research has indicated that KIFC3 might cap and deliver free MTs to their final destination (68). Remarkably, however, KIFC3 knockout mice are viable and develop normally (65), suggesting that other proteins may have overlapping roles or that other proteins can compensate for the role of KIFC3.

Finally, the Rab11 family interacting protein 3 (FIP3) displayed a high affinity to a construct containing a flagged version of FAM161A using the PLA assay. FIP3 is an effector protein of the small GTPase Rab11 (69) and localizes pericentrosomally during interphase (70) regulating the endosomal recycling compartment in collaboration with cytoplasmatic dynein (71,72). Importantly, overexpression of FIP3 in human epidermal carcinoma provokes fragmentation of the GA by sequestering cytoplasmatic dynein (73). In addition, FIP3 plays important roles in membrane trafficking (74). Notably, it has been proposed that FIP3 facilitates the trafficking of the photopigment rhodopsin in vesicles from the inner segment to the outer segments of the photoreceptors (75). According to this hypothesis, FIP3 could recognize the ciliary targeting motif in the rhodopsin sequence directly on the trans-Golgi network (75). Taken together, these data strongly support the involvement of FAM161A in functions related to the setting up of the MTOCs and transport of intracellular components through MTs as well as in the preservation of the physiology/homeostasis of photoreceptors.

In summary, our results show that a number of components of the newly discovered Golgi-centrosomal interactome are FAM161A's own partners, indicating that this protein is itself part of this network. FAM161A's functions are therefore probably

not limited to structural roles within the connecting cilium or the cytoskeleton, as originally thought, but likely extend to other processes, to be precisely characterized in further experiments, that are typical of other organelles.

Materials and methods

DNA constructs

All DNA constructs and plasmids for FAM161A were generated using the gateway system from Invitrogen, using the donor and destination plasmids described previously (27). The Flag-SOX4 plasmid was generously donated by Dr Luca Bartesaghi (University of Lausanne).

Yeast two hybrid

For Y2H analysis, we used a GAL4-based assay HybriZAP from Stratagene (La Jolla, CA, USA). Full-length FAM161A and partial constructs corresponding to N-term and to C-term of FAM161A were fused to a DNA-binding domain (GAL4-BD) and used as a bait to screen human and bovine retinal cDNA libraries. These were obtained by retrotranscribing RNA from fresh tissue using oligo-dT (human library) or random hexamers (bovine library), as primers. Both bait and prey plasmids, carrying the HIS3 (histidine), ADE2 (adenine), MEL1 (α-galactosidase) and LacZ (β-galactosidase) reporter genes, were used to transform the yeast strain PJ69-4A. Interactions were assessed by the activation of reporter genes, conferring the ability to grow in a selective media (depleted of histidine and adenine), and colorimetric assays (α-galactoside 'on plate' assay and β-galactoside filter lift assay) (76). A tip was used to collect traces of the colony and a colony PCR was performed using primers specific for the prey plasmid. Colony yielding no amplification products on the first attempt were re-picked and re-amplified for a maximum of three times. PCR products were then purified by the PCRclean kit from Millipore (Billerica, MA, USA) and sequenced using the BigDye terminator reagent v1.1 (Applied Biosystems, Life Technology, Foster City, CA, USA). Capillary electrophoresis was performed using the ABI 3130XL sequencer (Applied Biosystems), and electropherograms were analyzed using CLC Bio workbench v.5.0 (Qiagen, Hilden, Germany). The identity of the protein corresponding to the DNA sequence carried by the clone was identified by BLAST analysis (77).

Cell culture

HEK293T (human embryonic kidney) cells were grown under normal conditions using Dulbecco Modified Eagle Medium (DMEM) with Glutamax supplemented with bovine serum (10%), penicillin/streptomycin antibiotics (1%) and all of them purchased from Gibco (Carlsbad, CA, USA). hTERT-RPE1 cells were cultured using a mixture of 50% DMEM and 50% F12 supplemented with 10% bovine serum and 0.01 mg/ml hygromycin B (Gibco).

Immunostaining

For cell cycle immunostaining, cells were plated at low confluence on glass coverslip and after 24 h fixed in 100% methanol at −20°C for 15 min. After fixation, cells were washed twice with 1× phosphate-buffered saline pH 7.4 (PBS) and permeabilized with PBS containing 0.1% Triton X-100 for 10 min. Cells were then blocked for 1 h in blocking buffer (PBS with 2% bovine serum albumin). After overnight primary antibody incubation in blocking buffer, fixed cells were washed with PBS for three times, 5 min each. Cells were then incubated with secondary antibody linked to a specific fluorophore for 1 h at room temperature, washed three times with PBS and mounted on a glass slide using antifade mounting media Immumont (Thermo Scientific, Waltham, MA, USA). Images were captured using confocal scanning (see below).

Antibodies

To reveal the Flag-FAM161A constructs, we used either a mouse monoclonal anti-Flag antibody or a rabbit polyclonal anti-FAM161A from Sigma-Aldrich (St Louise, MO, USA). Rabbit polyclonal anti-NIN antibody (clone Poly6028) was purchased from Biolegends Inc. (London, UK). To reveal AKAP9, we used a rabbit polyclonal anti-AKAP9/GC-NAP antibody from Bethyl Lab (Montgomery, TX, USA) and mouse anti-AKAP9 (BD Biosciences, St Jose, CA, USA). Rabbit anti-GMAP210 and rabbit anti-KLC2 at both Bethyl Lab. Rabbit anti-GOLGA3, FIP3, KIFC3 and Myomegalin (PDE4DIP) were all purchased by GeneTex (Irvine, CA, USA). As the secondary antibody for immunoblotting, we used goat monoclonal anti-mouse IRDye 680 or goat monoclonal anti-rabbit IRDye 800 for Odyssey Infrared imaging system (LI-COR, Bad Homburg, Germany). For cell cycle immunostaining, rabbit polyclonal FAM161A antibody (Sigma-Aldrich), mouse monoclonal anti polyglutamylated tubulin (GT335, kindly provided by Dr Carsten Janke) were used as primary antibodies. Fluorophore-conjugated Alexa Fluor anti-mouse and anti-rabbit were used as secondary antibodies and were purchased from Life Technology (Carlsbad, CA, USA). A complete list of antibodies used is given in Supplementary Material, Table S5.

Immunoprecipitation

For immunoprecipitation (IP) experiments, HEK293T cells were grown to 70% confluence in a 150-cm dish and transfected with Jetprime reagent (Polyplus transfecting reagents, New York, NY, USA) with one of the four plasmids used for the assay (Flag-FAM161A, Flag-N-term-FAM161A, Flag-C-term-FAM161A, Flag-SOX4) (27). Cells were collected 24 h after transfection and lysed in IP extraction buffer [30 mM Tris–HCl (pH 7.4), 150 mM NaCl, 0.1% Triton X100 supplemented with fresh protease inhibitors]. Protein extract was then clarified by a 20-min centrifugation at 11 000*g* and the supernatant protein concentration quantified by using the Pierce BCA protein assay from Thermo Scientific. We used 2–4 mg of total protein extract for each assay. To immunoprecipitate flagged proteins, we used Flag-M2 agarose beads (Sigma-Aldrich) with overnight incubation. Beads were then washed four times with IP extraction buffer and incubated for 5 min on a rotating wheel during each wash. After washing, beads were boiled with loading buffer containing 1% β-mercaptoethanol for 5 min and then analyzed by sodium dodecyl sulfate polyacrylamide gel electrophoresis (SDS-PAGE) to separate different bands. To immunoprecipitate the native proteins of interest, 3 μg of respective antibody was incubated with Protein G Dynabeads (Life Technology) for 1 h on a rotating wheel. Following this, 2 mg of total lysate was incubated overnight with antibody-bound magnetic beads. Beads were then washed three times with IP extraction buffer by simple pipetting and the supernatant was discarded each time. Beads were finally incubated in loading buffer and boiled at 70°C for 10 min, prior to loading the supernatant directly on SDS-PAGE gels. For immunoblotting, proteins were transferred from polyacrylamide gels to nitrocellulose membranes and then incubated in blocking buffer (5% low-fat dry milk in 1 × Tris buffered saline Tween 0.1%—TBST) for 1 h.

Primary antibodies were incubated overnight in blocking buffer and then the membranes were washed 3 × 10 min in TBST followed by a 1-h incubation in secondary antibody blocking buffer (0.5% low-fat dry milk in TBST). Finally, following 3 × 10 min wash in TBST and a final 10 min wash in PBS, immunoblotting was revealed by an Odyssey Infrared imaging system (LI-COR) by exciting the fluorophore with 700 and 800 nm wavelength lights. Acquired two-channel images were then processed by Image Studio Lite software (LI-COR).

Proximity ligation assay

PLA allows detection of protein–protein interactions by exploiting space proximity of antibodies targeting putative interacting partners. In short, primary antibodies raised in different species are bound to target proteins on cell or tissue samples fixed on a microscope slide. Secondary species-specific antibodies conjugated with particular DNA sequences are then supplemented to the system, along with a 'connector' oligonucleotide, complementary to both sequences and DNA ligase. If target proteins interact (are proximal in space), a DNA loop is formed and incubation with a DNA polymerase allows rolling circle amplification of the loop. Complementary fluorescent probes are then added to the system and fluoresce is measured by microscopy. Interacting proteins are indeed visible as fluorescent signals, allowing not only detecting interaction but also (if needed) cellular localization.

To perform PLA, HEK293T cells were grown on 8 mm coverslips coated with poly-L-lysine hydrobromide. Cells were transfected with either Flag-FAM161A (full length) or with the plasmid backbone (p3Flag) as a negative control. Cells were seeded to reach around 80% confluence at the moment of fixation and transfected contextually using FuGENE (Promega, Madison, WI, USA) transfecting kit (8 μg of plasmidic DNA) according to manufacturer's instructions. Transfected cells were fixed in 4% paraformaldehyde in CB buffer (200 mM PIPES pH 6.8, 300 mM NaCl, 10 mM ethylene glycol tetraacetic acid pH 8.0, 10 mM glucose, 10 mM MgCl$_2$). Fixing solution was washed three times in CB buffer supplemented with 50 mM NH$_4$Cl. Cells were then permeabilized with PBS + 0.05% Triton X-100 applied for 5 min. After permeabilization, cells were blocked in blocking solution [from PLA kit, Olink (Uppsala, Sweden)] for 30 min at 37°C and incubated with primary antibodies of interest, in antibody diluent (from PLA kit) overnight at 4°C. The day after, cells were washed 3 × 5 min in CB buffer with gentle shaking and incubated with PLA probes diluted 1 : 5 in antibody diluent. Next, ligation mix (Ligation Stock 1:5 + Ligase 1:40 in high purity water) was added and incubated for 30 min at 37°C. Ligation mix was washed 2 × 2 min with gentle shaking. Amplification-Polymerase solution (Amplification Stock 1:5 + Polymerase 1 : 80 in high purity water) was incubated for 100 min at 37°C and finally washed in 1× wash buffer B (Tris–HCl 0.2 M, pH 7.5; NaCl 0.1 M) 2 × 10 min and in 0.01× wash buffer B for 1 min. Finally, cells were then incubated for 5 min in DAPI 1× dissolved in PBS, followed by 2 × 5 min in CB buffer, and 1 × 5 min wash in high purity water, and then mounted with Immumont (Thermo Scientific). Experiments were analyzed by confocal microscopy.

Confocal microscopy

Slides were observed using confocal scanning with a Zeiss LSM 710 Quasar Confocal microscope (Carl Zeiss, Jena, Germany), with oil immersion objective ×63, NA 1.4. For each channel, the pinhole was set to the Airy Unit corresponding to a width of 0.9 μm per sample. For each slide the Z-stack was acquired with an average corresponding to four passages and a sampling in the XYZ plains according to the criteria of Nyquist. Images were processed using Fiji (78) and Adobe Photoshop CS5 (Adobe Systems, San Jose, CA, USA).

Cells quantification

The resulting images were investigated using a script written in ImageJ macro language (http://rsbweb.nih.gov/ij/). Briefly, the script first processes the Z-stack with the Maximum Intensity Projection method, then it conveys the resulting image to a Gaussian Blur Filter (sigma = 1), a Rolling Ball Background Subtraction algorithm (radius = 10 pixels) and to a Water-Shedding algorithm. Following this, the images were segmented after calculating the threshold with the Max Entropy algorithm and the PLA foci were assessed using the Analyze Particle ImageJ function. The nuclei stained with DAPI were manually counted to quantify the number of cells in each acquisition. On average, 30–60 cells were acquired for each field.

Bioinformatic analyses

GO annotations were performed by using the Database for Annotation, Visualization and Integrated Discovery (DAVID) web interface from National Institute of Allergy and Infectious Disease, NIH (http://david.abcc.ncifcrf.gov) (35,36). The gene interaction network was generated using the GeneMANIA web interface from the University of Toronto (http://www.genemania.org) (34). Statistical analysis was performed using the Keisan online calculator (http://keisan.casio.com).

Supplementary material

Supplementary material is available at HMG online.

References

1. Rios, R.M. (2014) The centrosome–Golgi apparatus nexus. *Philos. Trans. R. Soc. B Biol. Sci.*, **369**, 20130462.
2. Zhu, X. and Kaverina, I. (2013) Golgi as an MTOC: making microtubules for its own good. *Histochem. Cell Biol.*, **140**, 361–367.
3. Chabin-Brion, K., Marceiller, J., Perez, F., Settegrana, C., Drechou, A., Durand, G. and Poüs, C. (2001) The golgi complex is a microtubule-organizing organelle. *Mol. Biol. Cell*, **12**, 2047–2060.
4. Hurtado, L., Caballero, C., Gavilan, M.P., Cardenas, J., Bornens, M. and Rios, R.M. (2011) Disconnecting the Golgi ribbon from the centrosome prevents directional cell migration and ciliogenesis. *J. Cell Biol.*, **193**, 917–933.
5. Efimov, A., Kharitonov, A., Efimova, N., Loncarek, J., Miller, P.M., Andreyeva, N., Gleeson, P., Galjart, N., Maia, A.R.R., McLeod, I.X. *et al.* (2007) Asymmetric CLASP-dependent

nucleation of noncentrosomal microtubules at the trans-golgi network. *Dev. Cell*, **12**, 917–930.

6. Colanzi, A., Suetterlin, C. and Malhotra, V. (2003) Cell-cycle-specific Golgi fragmentation: how and why? *Curr. Opin. Cell Biol.*, **15**, 462–467.

7. Singla, V. and Reiter, J. (2006) The primary cilium as the cell's antenna: signaling at a sensory organelle. *Science*, **313**, 629–633.

8. Goetz, S.C. and Anderson, K.V. (2010) The primary cilium: a signalling centre during vertebrate development. *Nat. Rev. Genet.*, **11**, 331–344.

9. Roy, S. (2009) The motile cilium in development and disease: emerging new insights. *Bioessays*, **31**, 694–699.

10. Takeda, S. and Narita, K. (2012) Structure and function of vertebrate cilia, towards a new taxonomy. *Differentiation*, **83**, S4–S11.

11. Drummond, I.A. (2012) Cilia functions in development. *Curr. Opin. Cell Biol.*, **24**, 24–30.

12. Hildebrandt, F., Benzing, T. and Katsanis, N. (2011) Ciliopathies. *N. Engl. J. Med.*, **364**, 1533–1543.

13. Waters, A. and Beales, P. (2011) Ciliopathies: an expanding disease spectrum. *Pediatr. Nephrol.*, **26**, 1039–1056.

14. Wright, A.F., Chakarova, C.F., Abd El-Aziz, M.M. and Bhattacharya, S.S. (2010) Photoreceptor degeneration: genetic and mechanistic dissection of a complex trait. *Nat. Rev. Genet.*, **11**, 273–284.

15. Estrada-Cuzcano, A., Roepman, R., Cremers, F.P.M., den Hollander, A.I. and Mans, D.A. (2012) Non-syndromic retinal ciliopathies: translating gene discovery into therapy. *Hum. Mol. Genet.*, **21**, R111–R124.

16. Hartong, D., Berson, E. and Dryja, T. (2006) Retinitis pigmentosa. *Lancet*, **368**, 1795–1809.

17. Berson, E. (1993) Retinitis pigmentosa. The Friedenwald Lecture. *Invest. Ophthalmol. Vis. Sci.*, **34**, 1659–1676.

18. Rivolta, C., Sharon, D., DeAngelis, M.M. and Dryja, T.P. (2002) Retinitis pigmentosa and allied diseases: numerous diseases, genes, and inheritance patterns. *Hum. Mol. Genet.*, **11**, 1219–1227.

19. Liu, Q., Zuo, J. and Pierce, E.A. (2004) The retinitis pigmentosa 1 protein is a photoreceptor microtubule-associated protein. *J. Neurosci.*, **24**, 6427–6436.

20. Hosch, J., Lorenz, B. and Stieger, K. (2011) RPGR: role in the photoreceptor cilium, human retinal disease, and gene therapy. *Ophthalmic Genet.*, **32**, 1–11.

21. Coene, K.L.M., Mans, D.A., Boldt, K., Gloeckner, C.J., van Reeuwijk, J., Bolat, E., Roosing, S., Letteboer, S.J.F., Peters, T.A., Cremers, F.P.M. *et al.* (2011) The ciliopathy-associated protein homologs RPGRIP1 and RPGRIP1L are linked to cilium integrity through interaction with Nek4 serine/threonine kinase. *Hum. Mol. Genet.*, **20**, 3592–3605.

22. El Shamieh, S., Neuillé, M., Terray, A., Orhan, E., Condroyer, C., Démontant, V., Michiels, C., Antonio, A., Boyard, F., Lancelot, M.-E. *et al.* (2014) Whole-exome sequencing identifies kiz as a ciliary gene associated with autosomal-recessive rod-cone dystrophy. *Am. J. Hum. Genet.*, **94**, 625–633.

23. Langmann, T., Di Gioia, S.A., Rau, I., Stöhr, H., Maksimovic, N.S., Corbo, J.C., Renner, A.B., Zrenner, E., Kumaramanickavel, G., Karlstetter, M. *et al.* (2010) Nonsense mutations in FAM161A cause RP28-associated recessive retinitis pigmentosa. *Am. J. Hum. Genet.*, **87**, 376–381.

24. Bandah-Rozenfeld, D., Mizrahi-Meissonnier, L., Farhy, C., Obolensky, A., Chowers, I., Pe'er, J., Merin, S., Ben-Yosef, T., Ashery-Padan, R., Banin, E. *et al.* (2010) Homozygosity mapping reveals null mutations in FAM161A as a cause of autosomal-recessive retinitis pigmentosa. *Am. J. Hum. Genet.*, **87**, 382–391.

25. Venturini, G., Di Gioia, S., Harper, S., Weigel-DiFranco, C., Rivolta, C. and Berson, E. (2014) Molecular genetics of FAM161A in North American patients with early-onset retinitis pigmentosa. *PLoS ONE*, **9**, e92479.

26. Duncan, J.L., Biswas, P., Kozak, I., Navani, M., Syed, R., Soudry, S., Menghini, M., Caruso, R.C., Jeffrey, B.G., Heckenlively, J.R. *et al.* (2014) Ocular phenotype of a family with FAM161A-associated retinal degeneration. *Ophthalmic Genet.*, 1–9.

27. Di Gioia, S.A., Letteboer, S.J.F., Kostic, C., Bandah-Rozenfeld, D., Hetterschijt, L., Sharon, D., Arsenijevic, Y., Roepman, R. and Rivolta, C. (2012) FAM161A, associated with retinitis pigmentosa, is a component of the cilia-basal body complex and interacts with proteins involved in ciliopathies. *Hum. Mol. Genet.*, **21**, 5174–5184.

28. Zach, F., Grassmann, F., Langmann, T., Sorusch, N., Wolfrum, U. and Stöhr, H. (2012) The retinitis pigmentosa 28 protein FAM161A is a novel ciliary protein involved in intermolecular protein interaction and microtubule association. *Hum. Mol. Genet.*, **21**, 4573–4586.

29. Roosing, S., Lamers, I.J., de Vrieze, E., van den Born, L.I., Lambertus, S. and Arts, H.H., POC1B_Study_Group, Peters, T.A., Hoyng, C.B., Kremer, H. *et al.* (2014) Disruption of the basal body protein POC1B results in autosomal-recessive cone-rod dystrophy. *Am. J. Hum. Genet.*, **95**, 131–142.

30. Karlstetter, M., Sorusch, N., Caramoy, A., Dannhausen, K., Aslanidis, A., Fauser, S., Boesl, M.R., Nagel-Wolfrum, K., Tamm, E.R., Jagle, H. *et al.* (2014) Disruption of the retinitis pigmentosa 28 gene Fam161a in mice affects photoreceptor ciliary structure and leads to progressive retinal degeneration. *Hum. Mol. Genet.*, **23**, 5197–5210.

31. van Reeuwijk, J., Arts, H.H. and Roepman, R. (2011) Scrutinizing ciliopathies by unraveling ciliary interaction networks. *Hum. Mol. Genet.*, **20**, R149–R157.

32. Gherman, A., Davis, E.E. and Katsanis, N. (2006) The ciliary proteome database: an integrated community resource for the genetic and functional dissection of cilia. *Nat. Genet.*, **38**, 961–962.

33. Boeckmann, B., Bairoch, A., Apweiler, R., Blatter, M.-C., Estreicher, A., Gasteiger, E., Martin, M.J., Michoud, K., O'Donovan, C., Phan, I. *et al.* (2003) The SWISS-PROT protein knowledgebase and its supplement TrEMBL in 2003. *Nucleic Acids Res.*, **31**, 365–370.

34. Mostafavi, S., Ray, D., Warde-Farley, D., Grouios, C. and Morris, Q. (2008) GeneMANIA: a real-time multiple association network integration algorithm for predicting gene function. *Genome Biol.*, **9**, S4.

35. Huang, D.W., Sherman, B.T. and Lempicki, R.A. (2008) Systematic and integrative analysis of large gene lists using DAVID bioinformatics resources. *Nat. Protoc.*, **4**, 44–57.

36. Huang, D.W., Sherman, B.T. and Lempicki, R.A. (2009) Bioinformatics enrichment tools: paths toward the comprehensive functional analysis of large gene lists. *Nucleic Acids Res.*, **37**, 1–13.

37. Sütterlin, C. and Colanzi, A. (2010) The Golgi and the centrosome: building a functional partnership. *J. Cell Biol.*, **188**, 621–628.

38. Barinaga-Rementeria Ramirez, I. and Lowe, M. (2009) Golgins and GRASPs: holding the Golgi together. *Semin. Cell Dev. Biol.*, **20**, 770–779.

39. Yadav, S., Puthenveedu, M.A. and Linstedt, A.D. (2012) Golgin160 recruits the dynein motor to position the golgi apparatus. *Dev. Cell*, **23**, 153–165.

40. Sorokin, S. (1962) Centrioles and the formation of rudimentary cilia by fibroblasts and smooth muscle cells. *J. Cell Biol.*, **15**, 363–377.

41. Follit, J., San Agustin, J., Xu, F., Jonassen, J., Samtani, R., Lo, C. and Pazour, G. (2008) The Golgin GMAP210/TRIP11 anchors IFT20 to the Golgi complex. *PLoS Genet.*, **4**, e1000315.

42. Rivero, S., Cardenas, J., Bornens, M. and Rios, R.M. (2009) Microtubule nucleation at the cis-side of the Golgi apparatus requires AKAP450 and GM130. *EMBO J.*, **28**, 1016–1028.

43. Roubin, R., Acquaviva, C., Chevrier, V., Sedjaï, F., Zyss, D., Birnbaum, D. and Rosnet, O. (2013) Myomegalin is necessary for the formation of centrosomal and Golgi-derived microtubules. *Biol. Open*, **2**, 238–250.

44. Rios, R.M., Sanchis, A., Tassin, A.M., Fedriani, C. and Bornens, M. (2004) GMAP-210 recruits gamma-tubulin complexes to cis-Golgi membranes and is required for Golgi ribbon formation. *Cell*, **118**, 323–335.

45. Witczak, O., Skalhegg, B.S., Keryer, G., Bornens, M., Tasken, K., Jahnsen, T. and Orstavik, S. (1999) Cloning and characterization of a cDNA encoding an A-kinase anchoring protein located in the centrosome, AKAP450. *EMBO J.*, **18**, 1858–1868.

46. Ou, Y.Y., Mack, G.J., Zhang, M. and Rattner, J.B. (2002) CEP110 and ninein are located in a specific domain of the centrosome associated with centrosome maturation. *J. Cell Sci.*, **115**, 1825–1835.

47. Stillwell, E.E., Zhou, J. and Joshi, H.C. (2004) Human Ninein is a centrosomal autoantigen recognized by CREST patient sera and plays a regulatory role in microtubule nucleation. *Cell Cycle*, **3**, 921–928.

48. Mogensen, M.M., Malik, A., Piel, M., Bouckson-Castaing, V. and Bornens, M. (2000) Microtubule minus-end anchorage at centrosomal and non-centrosomal sites: the role of ninein. *J. Cell Sci.*, **113**, 3013–3023.

49. Cheng, T.-S., Hsiao, Y.-L., Lin, C.-C., Hsu, C.-M., Chang, M.-S., Lee, C.-I., Yu, R.C.-T., Huang, C.-Y.F., Howng, S.-L. and Hong, Y.-R. (2007) hNinein is required for targeting spindle-associated protein Astrin to the centrosome during the S and G2 phases. *Exp. Cell Res.*, **313**, 1710–1721.

50. den Hollander, A.I., Koenekoop, R.K., Mohamed, M.D., Arts, H. H., Boldt, K., Towns, K.V., Sedmak, T., Beer, M., Nagel-Wolfrum, K., McKibbin, M. *et al.* (2007) Mutations in LCA5, encoding the ciliary protein lebercilin, cause Leber congenital amaurosis. *Nat. Genet.*, **39**, 889–895.

51. Chakarova, C.F., Khanna, H., Shah, A.Z., Patil, S.B., Sedmak, T., Murga-Zamalloa, C.A., Papaioannou, M.G., Nagel-Wolfrum, K., Lopez, I., Munro, P. *et al.* (2011) TOPORS, implicated in retinal degeneration, is a cilia-centrosomal protein. *Hum. Mol. Genet.*, **20**, 975–987.

52. Graser, S., Stierhof, Y.-D., Lavoie, S.B., Gassner, O.S., Lamla, S., Le Clech, M. and Nigg, E.A. (2007) Cep164, a novel centriole appendage protein required for primary cilium formation. *J. Cell Biol.*, **179**, 321–330.

53. Wang, C., Low, W.-C., Liu, A. and Wang, B. (2013) Centrosomal protein DZIP1 regulates hedgehog signaling by promoting cytoplasmic retention of transcription factor GLI3 and affecting ciliogenesis. *J. Biol. Chem.*, **288**, 29518–29529.

54. Conroy, P., Saladino, C., Dantas, T., Lalor, P., Dockery, P. and Morrison, C. (2012) C-NAP1 and rootletin restrain DNA damage-induced centriole splitting and facilitate ciliogenesis. *Cell Cycle*, **11**, 3769–3778.

55. Khateb, S., Zelinger, L., Mizrahi-Meissonnier, L., Ayuso, C., Koenekoop, R.K., Laxer, U., Gross, M., Banin, E. and Sharon, D. (2014) A homozygous nonsense CEP250 mutation combined with a heterozygous nonsense C2orf71 mutation is associated with atypical Usher syndrome. *J. Med. Genet.*, **51**, 460–469.

56. Oddoux, S., Zaal, K.J., Tate, V., Kenea, A., Nandkeolyar, S.A., Reid, E., Liu, W. and Ralston, E. (2013) Microtubules that form the stationary lattice of muscle fibers are dynamic and nucleated at Golgi elements. *J. Cell Biol.*, **203**, 205–213.

57. Wang, Z., Wu, T., Shi, L., Zhang, L., Zheng, W., Qu, J.Y., Niu, R. and Qi, R.Z. (2010) Conserved motif of CDK5RAP2 mediates its localization to centrosomes and the golgi complex. *J. Biol. Chem.*, **285**, 22658–22665.

58. Hoppeler-Lebel, A., Celati, C., Bellett, G., Mogensen, M.M., Klein-Hitpass, L., Bornens, M. and Tassin, A.-M. (2007) Centrosomal CAP350 protein stabilises microtubules associated with the Golgi complex. *J. Cell Sci.*, **120**, 3299–3308.

59. Hirokawa, N., Sato-Yoshitake, R., Kobayashi, N., Pfister, K.K., Bloom, G.S. and Brady, S.T. (1991) Kinesin associates with anterogradely transported membranous organelles in vivo. *J. Cell Biol.*, **114**, 295–302.

60. Butowt, R. and von Bartheld, C.S. (2007) Conventional kinesin-I motors participate in the anterograde axonal transport of neurotrophins in the visual system. *J. Neurosci. Res.*, **85**, 2546–2556.

61. Manser, C., Guillot, F., Vagnoni, A., Davies, J., Lau, K.F., McLoughlin, D.M., De Vos, K.J. and Miller, C.C.J. (2012) Lemur tyrosine kinase-2 signalling regulates kinesin-1 light chain-2 phosphorylation and binding of Smad2 cargo. *Oncogene*, **31**, 2773–2782.

62. Du, J., Wei, Y., Liu, L., Wang, Y., Khairova, R., Blumenthal, R., Tragon, T., Hunsberger, J.G., Machado-Vieira, R., Drevets, W. *et al.* (2010) A kinesin signaling complex mediates the ability of GSK-3β to affect mood-associated behaviors. *Proc. Natl Acad. Sci. USA*, **107**, 11573–11578.

63. Hong, Y.-R., Chen, C.-H., Chuo, M.-H., Liou, S.-Y. and Howng, S.-L. (2000) Genomic organization and molecular characterization of the human ninein gene. *Biochem. Biophys. Res. Commun.*, **279**, 989–995.

64. Bloom, G. and Endow, S. (1995) Motor proteins 1: kinesins. *Protein Profile*, **2**, 1105–1171.

65. Yang, Z., Xia, C.H., Roberts, E.A., Bush, K., Nigam, S.K. and Goldstein, L.S.B. (2001) Molecular cloning and functional analysis of mouse C-terminal kinesin motor KifC3. *Mol. Cell. Biol.*, **21**, 765–770.

66. Hoang, E., Bost-Usinger, L. and Burnside, B. (1999) Characterization of a novel C-kinesin (KIFC3) abundantly expressed in vertebrate retina and RPE. *Exp. Eye Res.*, **69**, 57–68.

67. Xu, Y., Takeda, S., Nakata, T., Noda, Y., Tanaka, Y. and Hirokawa, N. (2002) Role of KIFC3 motor protein in Golgi positioning and integration. *J. Cell Biol.*, **158**, 293–303.

68. Nachbar, J., Lázaro-Diéguez, F., Prekeris, R., Cohen, D. and Müsch, A. (2014) KIFC3 promotes mitotic progression and integrity of the central spindle in cytokinesis. *Cell Cycle*, **13**, 426–433.

69. Hales, C.M., Griner, R., Hobdy-Henderson, K.C., Dorn, M.C., Hardy, D., Kumar, R., Navarre, J., Chan, E.K.L., Lapierre, L.A. and Goldenring, J.R. (2001) Identification and characterization of a family of Rab11-interacting proteins. *J. Biol. Chem.*, **276**, 39067–39075.

70. Horgan, C.P., Walsh, M., Zurawski, T.H. and McCaffrey, M.W. (2004) Rab11-FIP3 localises to a Rab11-positive pericentrosomal compartment during interphase and to the cleavage furrow during cytokinesis. *Biochem. Biophys. Res. Commun.*, **319**, 83–94.

71. Horgan, C.P., Oleksy, A., Zhdanov, A.V., Lall, P.Y., White, I.J., Khan, A.R., Futter, C.E., McCaffrey, J.G. and McCaffrey, M.W. (2007) Rab11-FIP3 is critical for the structural integrity of the endosomal recycling compartment. *Traffic*, **8**, 414–430.

72. Horgan, C.P., Hanscom, S.R., Jolly, R.S., Futter, C.E. and McCaffrey, M.W. (2010) Rab11-FIP3 links the Rab11 GTPase and

cytoplasmic dynein to mediate transport to the endosomal-recycling compartment. *J. Cell Sci.*, **123**, 181–191.

73. Horgan, C.P., Hanscom, S.R., Jolly, R.S., Futter, C.E. and McCaffrey, M.W. (2010) Rab11-FIP3 binds dynein light intermediate chain 2 and its overexpression fragments the Golgi complex. *Biochem. Biophys. Res. Commun.*, **394**, 387–392.

74. Fielding, A.B., Schonteich, E., Matheson, J., Wilson, G., Yu, X., Hickson, G.R., Srivastava, S., Baldwin, S.A., Prekeris, R. and Gould, G.W. (2005) Rab11-FIP3 and FIP4 interact with Arf6 and the Exocyst to control membrane traffic in cytokinesis. *EMBO J.*, **24**, 3389–3399.

75. Wang, J. and Deretic, D. (2014) Molecular complexes that direct rhodopsin transport to primary cilia. *Prog. Retin. Eye Res.*, **38**, 1–19.

76. Letteboer, S. and Roepman, R. (2008) In Thompson, J., Ueffing, M. and Schaeffer-Reiss, C. (eds), *Functional Proteomics*. Humana Press, Totowa, New Jersey, 484, 145–159.

77. Altschul, S., Gish, W., Miller, W., Myers, E. and Lipman, D. (1990) Basic local alignment search tool. *J. Mol. Biol.*, **215**, 403–410.

78. Schindelin, J., Arganda-Carreras, I., Frise, E., Kaynig, V., Longair, M., Pietzsch, T., Preibisch, S., Rueden, C., Saalfeld, S., Schmid, B. *et al.* (2012) Fiji: an open-source platform for biological-image analysis. *Nat. Methods*, **9**, 676–682.